Paper for conference on Dynamic Positioning and Mooring of Floating Offshore Structures, organised by the Norwegian Society of Chartered Engineers, Kristiansand, September 2001.

Risk-Based Inspection Planning for Permanent Mooring Lines

Jan Mathisen,

Det Norske Veritas
Veritasveien 1,
N-1322 Høvik
(Jan.Mathisen@dnv.com)

1 Introduction

Reliability analysis of mooring lines in the DEEPMOOR joint industry project (ref. Mathisen, 1999a) forms some of the background for the present work. Considerable experience was gained in analysis of ultimate, accidental and fatigue limit states, and in using these results to calibrate the design rules for mooring lines, presented by Okkenhaug (2001). Although inspection methods for mooring lines were not addressed in this project, it seemed that they were empirically based, and might benefit from systematic analysis. At the same time, risk-based inspection planning has been applied to jackets, semisubmersibles, and floating production systems, as described by Sigurdsson et al. (2000). The present work describes a first attempt to apply risk-based inspection planning to mooring chain.

The main challenges in the analysis are to provide a realistic model for probabilistic crack-growth in a single chain link, and to take a large number of chain links into account, with a realistic correlation between links. The result of the analysis is a plan stating when it is cost-optimal to inspect the chain. Some results are shown for chain from a turret-moored ship in Norwegian waters. The uppermost chain segment in the most heavily loaded mooring line is considered. This chain has been conservatively designed, with a fatigue safety factor of 10. The present example is intended to illustrate the method without providing full details of the case study.

2 Method

2.1 Fatigue Loading

The fatigue loading of mooring chain is generally taken to be due to the tension cycles induced in the chain by;

- low-frequency platform motions in a horizontal plane, due to wind gusts and 2nd order wave loads, and
- wave-frequency motion of the platform with 6 degrees of freedom due to 1st order wave loads.

The magnitude of the tension cycles is also dependent on the mean tension in the line, due to pretension and mean environmental loads.

Standard methods are available to compute the fatigue damage due to these tension cycles under the Miner-Palmgren hypothesis, as described in DNV's OS-E301, or API RP 2SK. In the present case, intermediate results from the fatigue analysis made during the mooring line design are used to establish a long-term distribution of tension ranges. A Weibull distribution function is fitted to this data. This distribution function may be written

$$F_P(\Delta p) = 1 - \exp\left\{-\left(\frac{\Delta p}{a}\right)^b\right\} \qquad \textbf{(1)}$$

where Δp is the magnitude of a tension range (peak to trough), a is the scale parameter of the distribution and b is the exponent parameter of the distribution. It applies to the most heavily-loaded mooring line, and effectively includes both low-frequency and wave-frequency effects, with a mean period of 14 s.

2.2 Crack Growth Model for Chain Fatigue

2.2.1 Crack growth

Cracks are assumed to grow from the surface of a chain link, with a semi-elliptical shape, as indicated in Fig. 1, where *a* is the crack depth and (lower case) *c* is half the crack length.

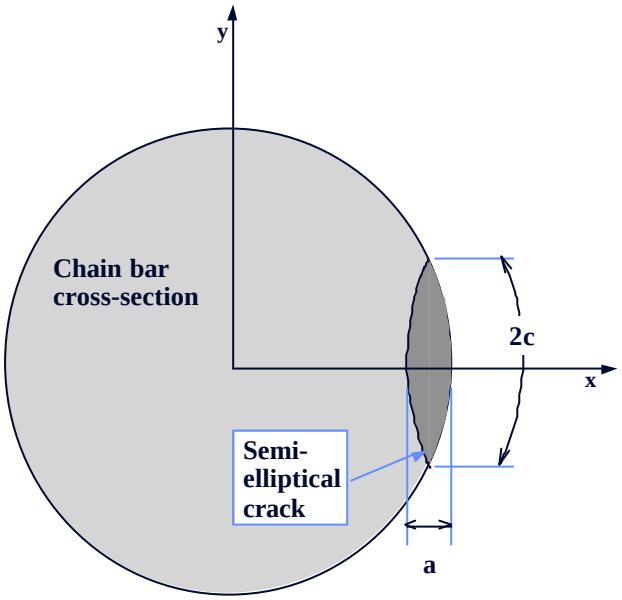

Figure 1 Crack size.

The crack growth is modelled by linear fracture mechanics, using the Paris-Erdogan equation in the 2-dimensional form:

$$\frac{da}{dN} = C(\Delta K_A)^m ; \quad \Delta K_A > \Delta K_{th} \quad ; \quad a(N_0) = a_0 \tag{2}$$

$$\frac{dc}{dN} = C(\Delta K_C)^m ; \quad \Delta K_C > \Delta K_{th} \quad ; \quad c(N_0) = c_0 \tag{3}$$

These equations provide the increment in the crack depth and crack half-length from one tension cycle, where *N* represents the number of tension cycles. The subscripts, A and C, refer to the deepest point of the crack, and to an end point of the crack at the surface, respectively. m and (upper case) C are material parameters, and are taken from BS7910. ΔK_A and ΔK_C are applied stress intensity ranges at the two locations indicated by the subscripts. ΔK_{th} is a stress intensity threshold, below which no crack growth takes place. This threshold is not applied in the present analysis; i.e. it is effectively zero. $a(N_0)$ indicates the initial crack depth before any load cycles have been applied; i.e. at $N = N_0$, and $c(N_0)$ indicates the initial half-length of the crack.

A finite element analysis has been carried out to determine the local stresses due to the applied tension, in an intact, studless, chain link. The stress distributions have been established for 3 cross-sections located at the weld, in the bend, and at the crown of the link. A sample stress distribution is shown in Figure 2. Standard practice in crack growth analysis, based on BS7910, is to linearise the actual stress distribution using a combination of membrane and bending stress components, as indicated in Figure 3.

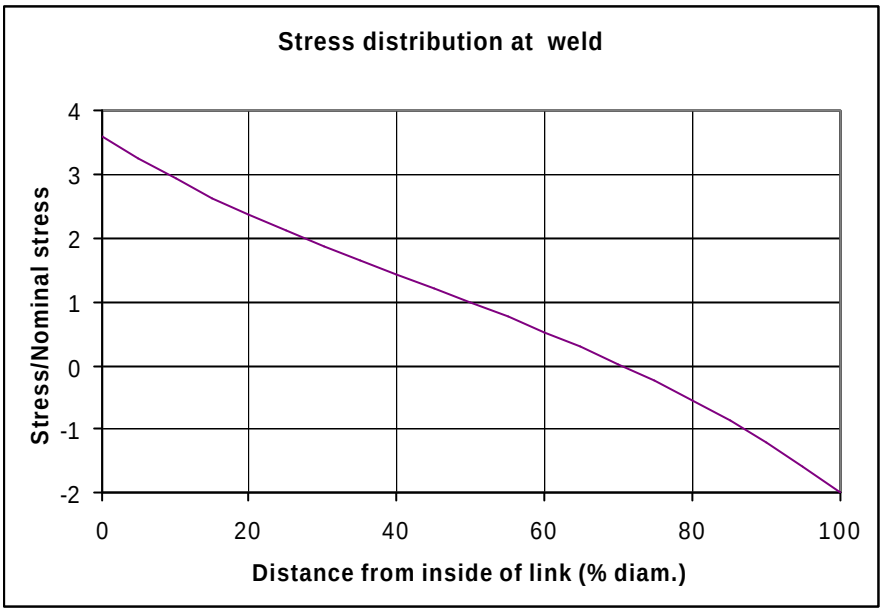

Figure 2 Stress distribution over a cross-section through weld for an intact link.

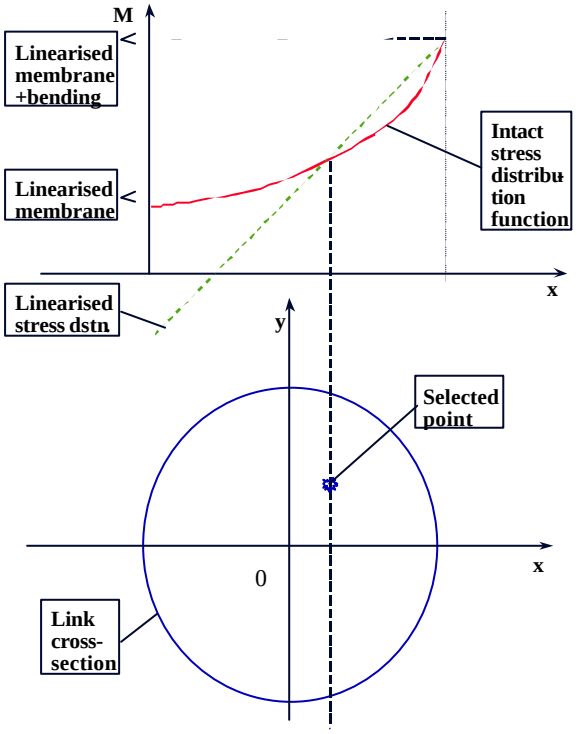

Figure 3 Linearisation of stress distribution over a selected cross-section through an intact link.

The stress intensity ranges applied in equations (2) and (3) are taken as the sums of the stress intensity ranges due to membrane (subscript *m*) and bending (subscript *b*) stresses. The stress intensity range for either membrane or bending stress is obtained by

$$\Delta K_{ij} = \Delta s_{j}(x) \cdot Y_{ij}(a,c) \cdot \sqrt{pa}\ , \quad i = A,C, \quad j = m,b \qquad \textbf{(4)}$$

where index $i=A$ indicates the crack tip at the deepest point and index $i=C$ is for the crack tip on the surface, index $j=m$ indicates membrane stress and index $j=b$ is for bending stress, Δs is a stress range, and $Y(a,c)$ is a geometry function that takes account of the effect of the presence of the crack on the stress distribution. In the present analysis, we are assuming that the crack propagates symmetrically with respect to the x-axis in Figure 3. This implies the same crack growth at both ends of the crack on the surface, and that the deepest point of the crack lies on the x-axis. Cracks may start from defects away from the x-axis, but will tend to align themselves in this way as they grow larger, according to Pommier et al. (1999).

Numerical geometry functions developed by Klasen and Dillstrom (2001) are applied in the present analysis. Their results have been extended down to infinitesimal crack size using results from Pommier et al. (1999). An example is given in Figure 4, showing good agreement with a collection of data for this type of geometry functions by Coroneau (1998).

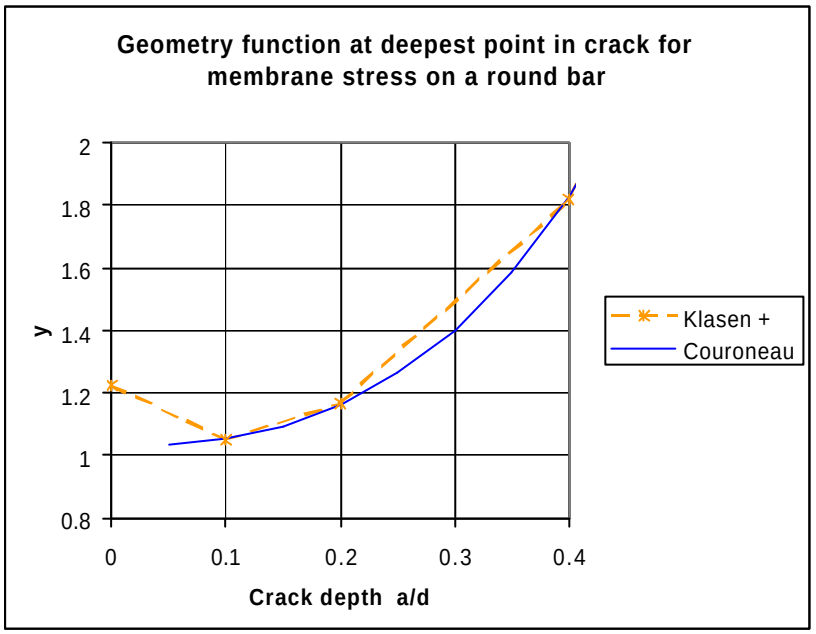

Figure 4 Example of geometry function (for a straight flaw), compared to Couroneau (1998).

2.2.2 Critical crack depth

The link is defined to fail when the crack depth reaches the critical crack depth. The critical crack depth is calculated as the crack depth that will just lead to rupture when the line tension level corresponds to a return period of 1 year. This line tension is obtained from the original design analysis of the mooring system. A level 2A failure assessment diagram (FAD) from BS7910 is used to calculate the critical crack size. The fracture toughness of the link material is needed for the FAD, and is obtained from the Charpy V impact tests carried out during the production of the chain links. The yield strength and ultimate tensile strength are also taken from the chain production test data. The following critical crack depths are obtained:

12% of chain diameter at weld section,

30% of chain diameter at bend section,

15% of chain diameter at crown section.

The weld section has the lowest fracture toughness, while the outer part of the crown section has the highest nominal tensile stress level .

The initial condition of the chain is assumed to be as it is immediately after production, corresponding to the test links that are used in S-N tests. The mean value of the initial crack size in the crack growth model is deterministically calibrated to provide the same time to failure as given by S-N analysis, using the logarithmic mean value of the K-parameter of the S-N curve. This parameter is taken from an S-N curve that Mathisen et al. (1999b) have fitted to data including some results from the joint industry study on Studless Chain Fatigue, organised by Noble Denton and Associates Inc., with testing by the National Engineering Laboratory. These data apply specifically to R4 grade studless chain in a salt water environment. The linear fracture mechanics model does not normally include the crack initiation phase. With this calibration method, the crack initiation phase is inserted in the model by applying very small initial crack sizes. Furthermore, consistency with this calibration principle implies consideration of a single crack location in each chain link. The weld section is chosen for the crack location in this analysis.

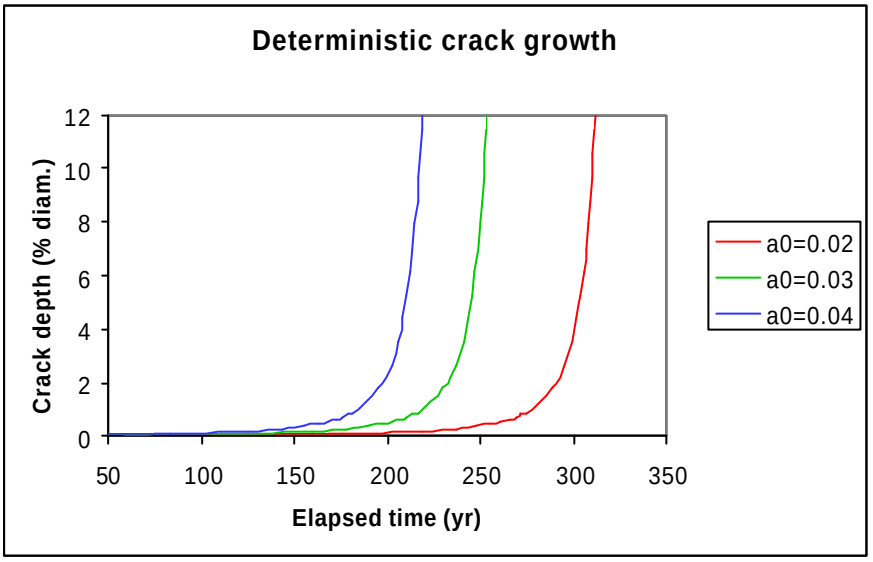

Figure 5 Deterministic crack growth with initial crack depths 0.02, 0.03, 0.04 mm.

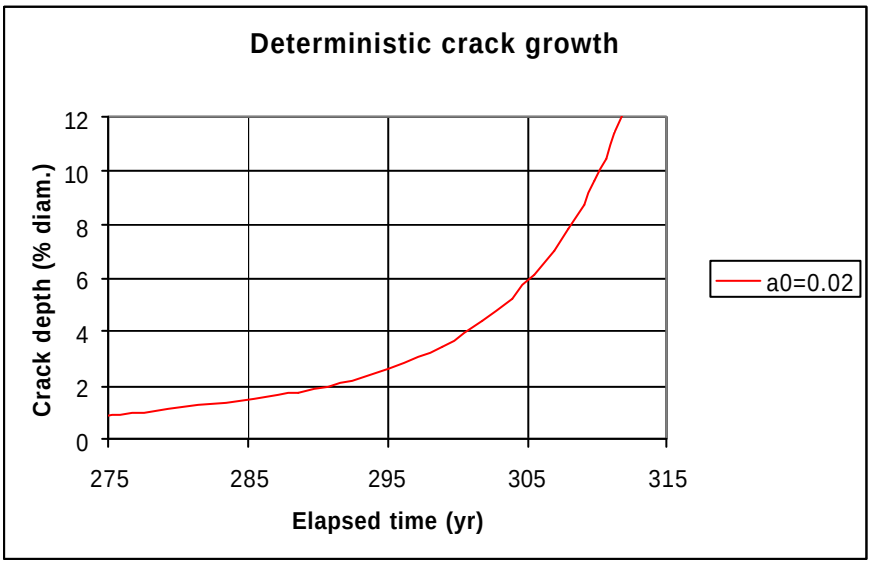

Figure 6 Latter part of deterministic crack growth with initial crack depth 0.02 mm.

Examples of deterministic crack growth curves are shown in Figure 5 and Figure 6, obtained by integrating equations (2) and (3) with fairly representative parameters. The time to critical crack size is long, but is sensitive to variation in the initial crack size. The crack initiation phase is long, followed by relatively rapid crack growth. The case in Figure 6 shows a crack size that might be detected if the link were inspected during the 30 year interval before critical crack size.

2.2.3 Reliability Analysis of a Single Link

The link failure event is defined to take place when the crack depth exceeds the critical crack depth. The following stochastic variables are included in the analysis:

(a) the scale parameter of the Weibull distribution of tension ranges, used to model load model uncertainty, with a normal distribution and 15% coefficient of variation (CoV),

(b) the variability in the material parameter, as a normal variable, with CoV based on BS7910,

(c) the model uncertainty in the geometry function, as a normal variable with 5% CoV,

(d) the initial crack depth, with exponential distribution,

(e) the aspect ratio of the initial crack a_0/c_0, as a normal variable with 10% CoV,

2.2.4 Reliability Analysis of a Chain Segment

The chain segment fails when the largest crack in all the links in the segment exceeds the critical crack size. It is essential to provide an appropriate level of stochastic dependency between the individual links in order to obtain meaningful reliability results for the chain segment. This often referred to as correlation between the links. The present approach is to define:

- some stochastic variables as global variables that are common to all links,
- some stochastic variables as local variables that are independent between the links, and
- to split some variables into global and local parts.

Since, the same tension is experienced by the whole chain segment (to a good approximation), the load model uncertainty is taken to be a global variable. The initial crack depth and aspect ratio are taken to be local variables. The material parameter *C* and the uncertainty in the geometry function are both split into global and local parts, with half the original variance in each part.

This segment model is based on judgement and some experience. It would be desirable to have a better basis in empirical data for the modelling of the dependency between the links. It turns out that the variability of the initial crack size is a dominant effect in the present analysis, as might be expected from Figure 5, so that the independence of this variable between links is a key assumption, while other details of the dependency between links appear to be less important.

The reliability calculation is nested in two layers, where the inner layer handles a conditional probability, conditioned with respect to the global variables. Integration over the probability distribution of the global variables is carried out in the outer layer. The number of links are taken into account between these two steps. The first order reliability method (FORM) is applied in the reliability calculations, using the PROBAN program (Sesam, 1996).

2.3 Inspection

2.3.1 Inspection and Repair Procedure

The chain segment is inspected ashore, after being replaced by a spare segment. Magnetic particle inspection (MPI) is applied. Only a sample of the links in the chain are normally inspected by MPI. 5% of the links are generally inspected, with 100% inspection in some parts, such as chain on windlasses or fairlead. Crack indications are often found on initial inspection. If these crack indications disappear after very light surface grinding then they are disregarded, as being due to inadequate surface preparation. Further grinding may be applied to repair cracks, to a maximum depth of 7% of the chain diameter. Larger cracks are repaired by replacing the chain link or the entire chain segment. The dimensions of detected cracks are not normally measured. The present chain segment has been inspected once after 3 years in service, without any cracks being detected.

2.3.2 Inspection Accuracy

The accuracy of the inspection technique is defined in terms of a probability of detection (PoD) curve. A PoD curve for common Nordic industrial practice, taken from Førli (2000), is assumed to be applicable. The curve is shown in Figure 7. The original curve provides a small probability of detecting very small defects, that is unrealistic, but usually of no importance. The present application is sensitive to this approximation, because the inspection is applied many times – to a large number of links. A lower limit has been introduced to the curve at 0.3 mm defect depth to reduce this sensitivity.

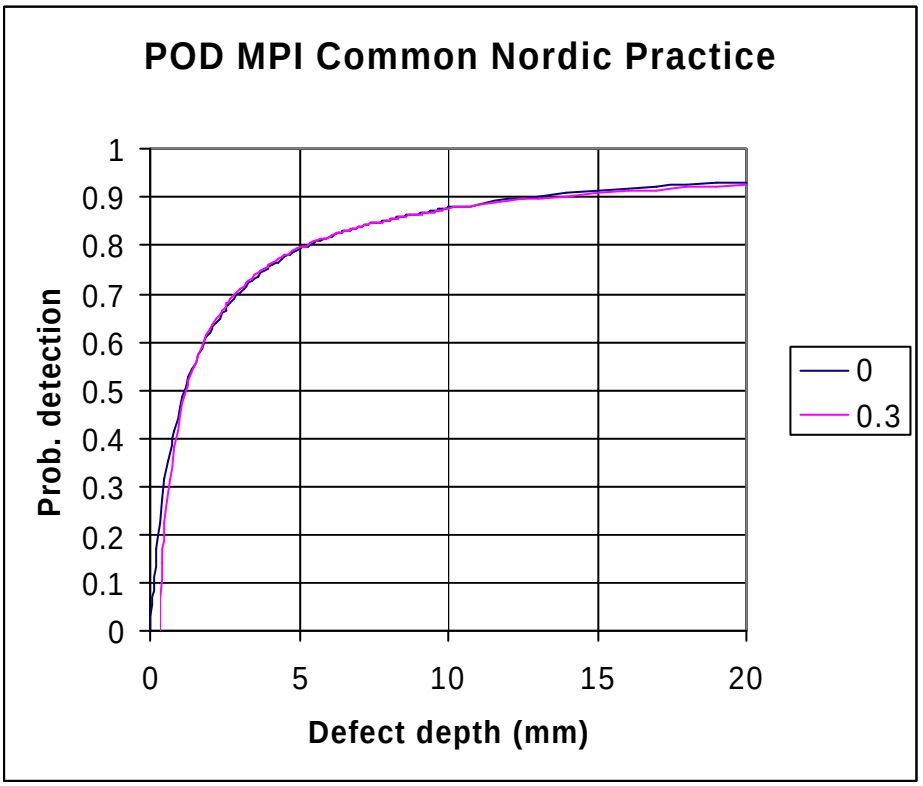

Figure 7 Probability of detection curve, with lower limits for defect depth of 0 and 0.3 mm.

2.3.3 Reliability Updating for One Chain Link from Inspection

Let us denote the event of fatigue failure in one link before time *t* by $E(F1,t)$. The probability of this event is computed as explained in section 2.2.3.

Next, let us denote the event of no detected crack in one link, from inspection at time t_i, by $E(I1,t_i)$. The probability of this event is computed as the probability that the crack size is less than the detectable crack size, where the latter is a stochastic variable drawn from the PoD curve.

The probability of failure can then be updated by expressing it as a conditional probability, which is computed from the probability of the intersection of the 2 events (both events take place), divided by the probability of the conditioning event

$$P\left[E(F1,t)\middle|E(I1,t_i)\right]=\frac{P\left[E(F1,t)\bigcap E(I1,t_i)\right]}{P\left[E(I1,t_i)\right]} \qquad \textbf{(5)}$$

This type of reasoning can be extended to include several inspections at different times, by including additional inspection events.

2.3.4 Reliability Updating for a Chain Segment from Inspection

The probability of chain segment failure can also be updated from inspection results, by extension of the expression in equation (5). In principle, the number of events considered has to be extended to include the failure events for all links, and the no-find events for all links that are inspected. Care has to be taken to insure that each link is treated consistently, so that the same stochastic variables are considered for failure and inspection events of that link. It is also advisable to reformulate in terms of the complementary events of link survival rather than link failure, since the survival event for the chain segment is provided by the intersection of survival events for all the links.

Only the no-find event is considered from inspections in the present analysis. This is the most likely type of event for a chain which is conservatively dimensioned with respect to fatigue. The other, most relevant, inspection event would be that a crack has been detected – a find event. Find events can, in principle, occur at any inspection, and in any number of inspected links. It is impractical to consider all possible combinations of no-find and find events when developing an inspection plan early in the life of a mooring system. However, if cracks are found later, then the inspection plan can be revised on the basis of these events.

2.4 Costs

Typical inspection costs are expected to lie in the range from MNOK 4 to MNOK 8. These costs are dominated by hire costs for a chain handling vessel, to retrieve the chain segment for inspection, and insert the replacement segment. The cost of the actual MPI is a marginal part of the inspection cost.

Repair costs are not relevant because only no-find events are taken into account from the inspections. Simple grinding repairs of occasional, small cracks would not add any significant cost.

The cost of a single line failure is estimated to be about 20 MNOK. This includes the cost of a replacement chain segment, installation of this segment, and the expected cost of lost production due to a reduced production window while one line is missing. Hence the ratio between single line failure cost and inspection cost lies in the range from 2.5 to 5.

If mooring system failure cost is considered, then the cost ratio may be as much as 3500. Mooring system failure is not usually expected to be a probable consequence of a single fatigue failure. However, if the initial rupture of a link with a fatigue crack occurs in severe weather, and a neighbouring line is about as highly utilised in fatigue, then rupture of a fatigued link in that neighbouring line may follow. This situation may lead to mooring system failure, if the weather is severe enough.

A discount rate of 6% p.a. is applied in the cost analysis.

2.5 Optimisation

The analysis is based on a cost optimisation, including:

- inspection cost,
- failure risk cost.

Repair cost is negligible in the present case.

A number of trial inspection plans are formulated, and the total costs are computed for each plan. The cost-optimal plan is found by selecting the trial plan that leads to the lowest costs. Each trial inspection plan is set up for a different target probability level, and inspections are applied when the probability of failure exceeds the target level.

Each inspection plan is considered in turn. The inspection cost is a simple deterministic function of the trial inspection plan. The updated probability of mooring line failure is also predicted, assuming that no cracks are detected at the planned inspections. The failure risk cost is taken as the costs associated with the fatigue failure of one mooring line, multiplied by the probability of failure.

3 Results

3.1 Single Link

The probability of failure of a single link is shown in Figure 8. This is the basic reliability calculation and form of presentation in the present paper, so it may be worthwhile to include some detailed comments. The time axis shows the elapsed time in years since the chain entered service. The probability axis shows the probability of failure, where failure is defined as a crack growth exceeding the critical crack depth at the weld location in the chain link. A logarithmic axis is applied to the probability. Most of the curves show the accumulated probability of failure over all elapsed years from the start of service. In some cases the annual probability of failure is also shown, as the increase in accumulated probability of failure during the last year.

The probability of link failure is very small initially, and increases gradually with time. Note that there is no allowance for surface defects introduced in the transportation, installation, or operation of the chain in these results. The annual probability of failure of a single link is quite low, even at the end of the design life.

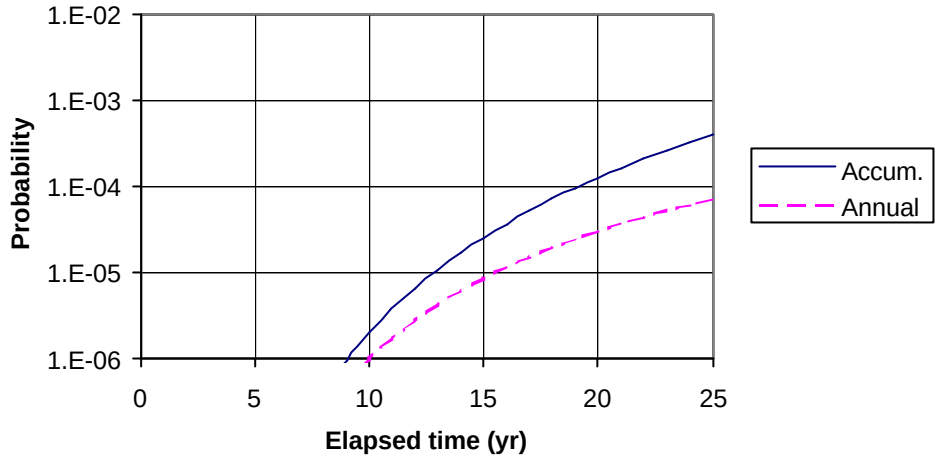

Figure 8 Probability of failure of a single link

Some conditional probability results are shown in Figure 9, showing how inspection with no crack found reduces the probability of failure. The probability of failure is reduced immediately after the inspection, but the effect of the inspection decreases as the time after the inspection continues to increase. Some reasons for the effect of the inspection can perhaps be explained as follows:

- Our initial knowledge of the fatigue behaviour of the chain link is based on a rather general capacity distribution, which usually implies considerable uncertainty. Inspection of the link with no defect found indicates that some of the more unfavourable possibilities contained in the capacity distribution are not realised in the present link.
- Furthermore, since no defect is detected, the crack growth model indicates that failure of the link is improbable in the near future.

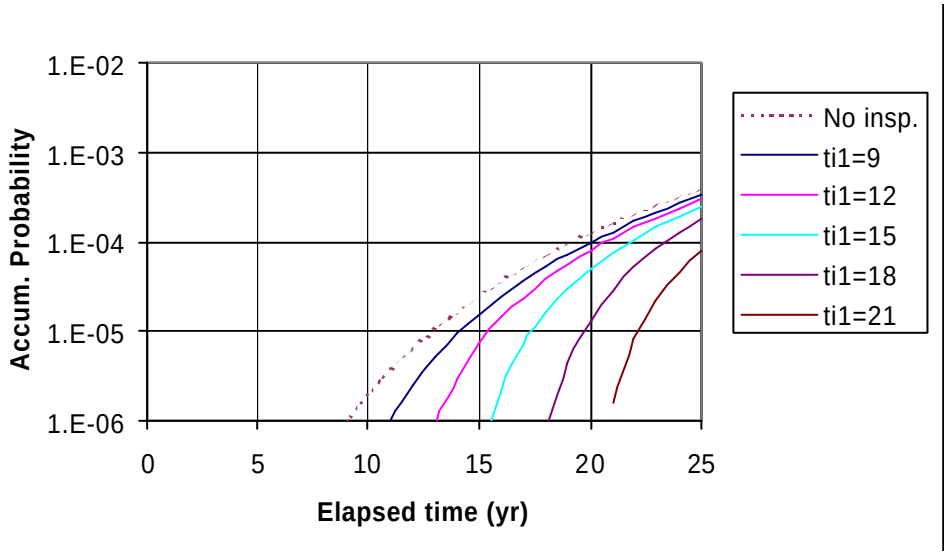

Figure 9 Probability of failure of a single link, conditional on inspection with no crack detected, at time t_{i1}.

3.2 Chain Segment

The top chain segment has 154 links under tension between the fairlead and the adjacent wire rope segment. The basic result for the probability of failure of the segment is shown in Figure 10. Due to a conservative fatigue design, there is only an accumulated probability of failure of 0.02 by the end of the design life – fatigue failure is fairly unlikely, but not highly improbable. The annual probability of failure at the end of the design life is 4×10^{-3}.

A comparison of link and segment probabilities of failure is also shown in this figure. The segment is 61 times more likely to have failed than the link by the end of the design life. This ratio is a consequence of the correlation between links that is implicit in the present analysis model. It shows that the correlation is low. Since the correlation is low, it follows that inspection of one link does not yield a confident assessment of the condition of another link. Furthermore, there is a relatively small number of chain links in the present chain segment, and the increase in cost of inspecting all the links is marginal. On this basis, it was decided **to base the inspection plan on MPI of each individual link**.

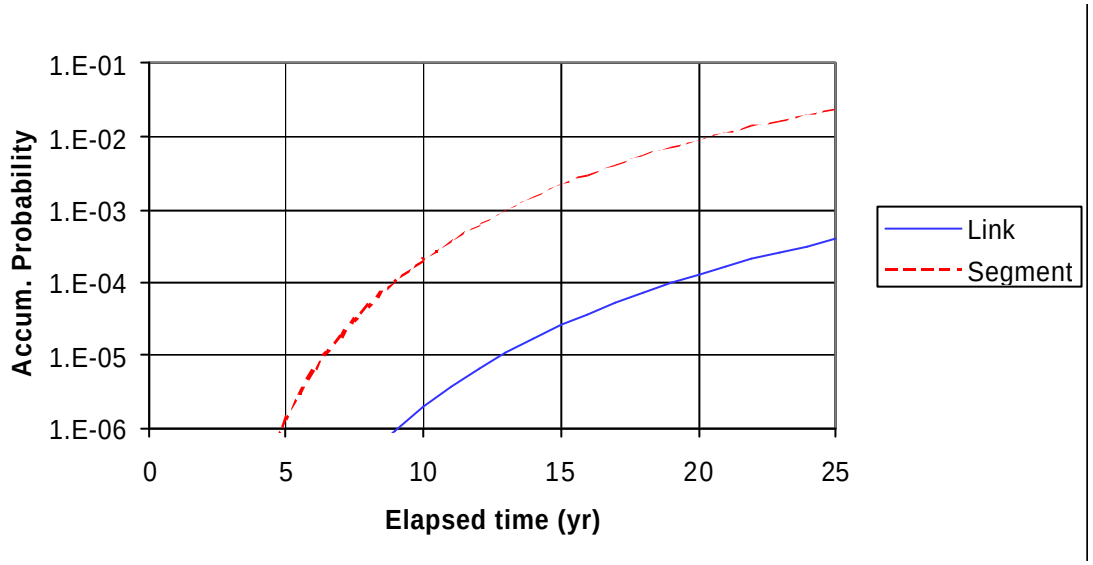

Figure 10 Comparison of accumulated probability of failure for a single link and a chain segment.

3.3 Inspection

A large number of parameter studies on the effects of inspection are needed for the optimisation of an inspection plan. A few examples are shown in this section. It is assumed that all the links in the chain segment are inspected at each inspection, and that no cracks are found in any links. The probability of failure is given conditional on these inspection events, based on generalisation of the expression in equation (5).

The effect of a single inspection on the probability of failure of the chain segment is shown in Figure 11, for inspections after 5, 10, 15 or 20 years. The uppermost curve in this figure shows the probability of failure with no inspection. The probability of failure is significantly reduced after an inspection with no-finds. In subsequent years, the probability of failure tends to increase, and gradually approach the curve for no inspections. Results of this type are developed for a single inspection in all years from year 3 to year 25.

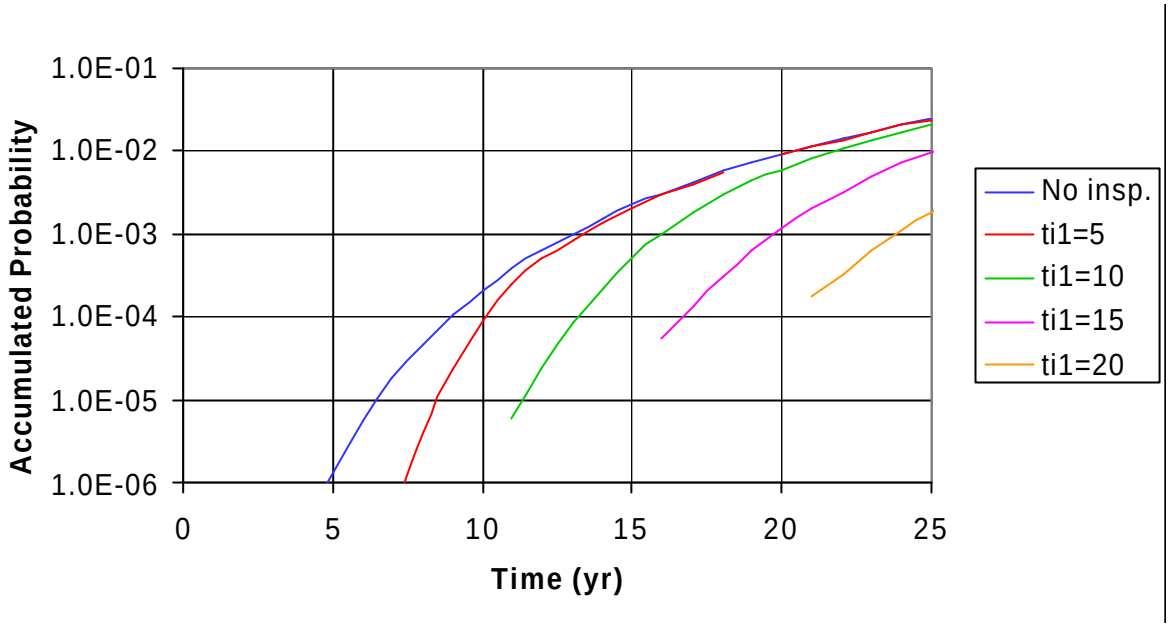

Figure 11 The effect of one inspection, with no-finds in all links, on the probability of failure, for inspections after 5, 10, 15, or 20 years.

The effect of two inspections is shown in Figure 12. The 1st inspection is in year 13 and the 2nd inspection in any year from year 14 to year 17. The same general effect is seen for the 2nd inspection as for the first inspection. There is a little irregularity in some of the curves for the second inspection, in the 1st year or two after the inspection. This is due to numerical difficulties in computing these problems more accurately. Fortunately, the general trend is very regular, and these curves can be faired manually by comparison with adjacent curves, if necessary. The curves are also manually extrapolated back to the year of inspection, for use in the inspection planning. Similar results are computed for 2nd inspections in every year between initial inspections and the end of the design life.

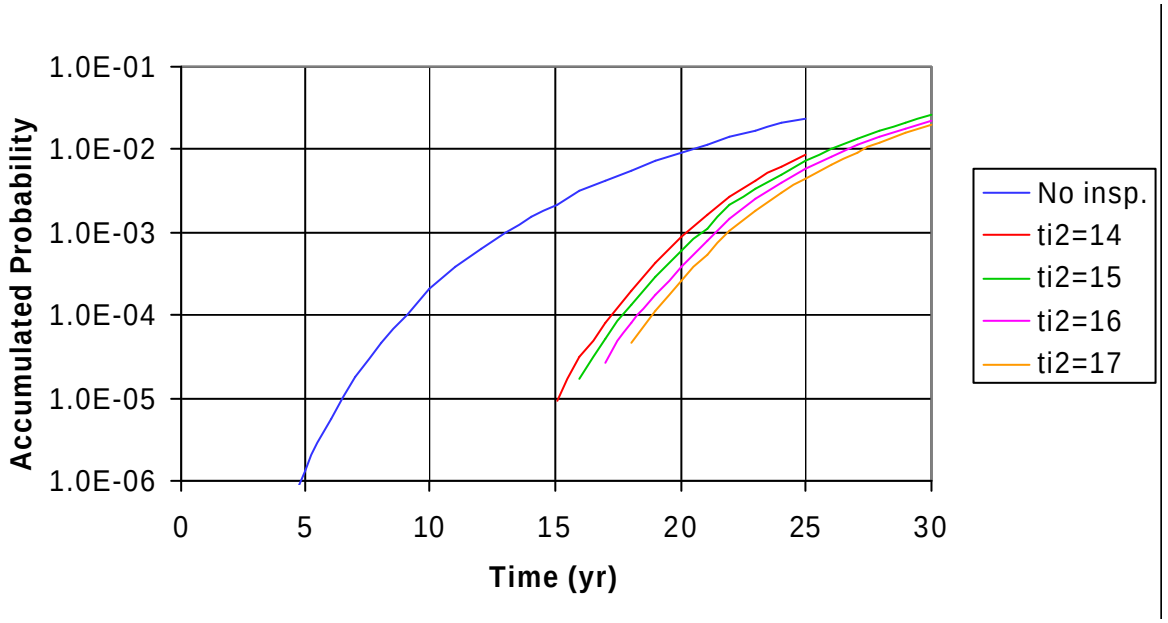

Figure 12 The effect of two inspections, with no-finds in all links, on the probability of failure, for the second inspection after 14, 15, 16, or 17 years, with the first inspection after 13 years.

Figure 13 shows how these results may be utilised in establishing an inspection plan. In this example, a target probability of failure of 10^{-3} is selected to determine the plan. The curve for the probability of failure with no inspections is followed until this target probability is exceeded, after 13 years. The first inspection is applied then. Provided no cracks are detected, the probability of failure drops, and the curve for one inspection at 13 years is followed, until the target probability is again exceeded, after 18 years. A second inspection is then applied. Again, provided no cracks are detected, the probability of failure drops, and the curve for a second inspection at 18 years is followed until the target is exceeded after about 23 years. A 3rd inspection would be applied then, but this is not shown on the figure.

The target probability is an accumulated probability in this example, but an annual probability is often applied instead. The application of a target probability in this way is an effective way of controlling the risk cost of failure; i.e. the probability of failure multiplied by the cost of failure.

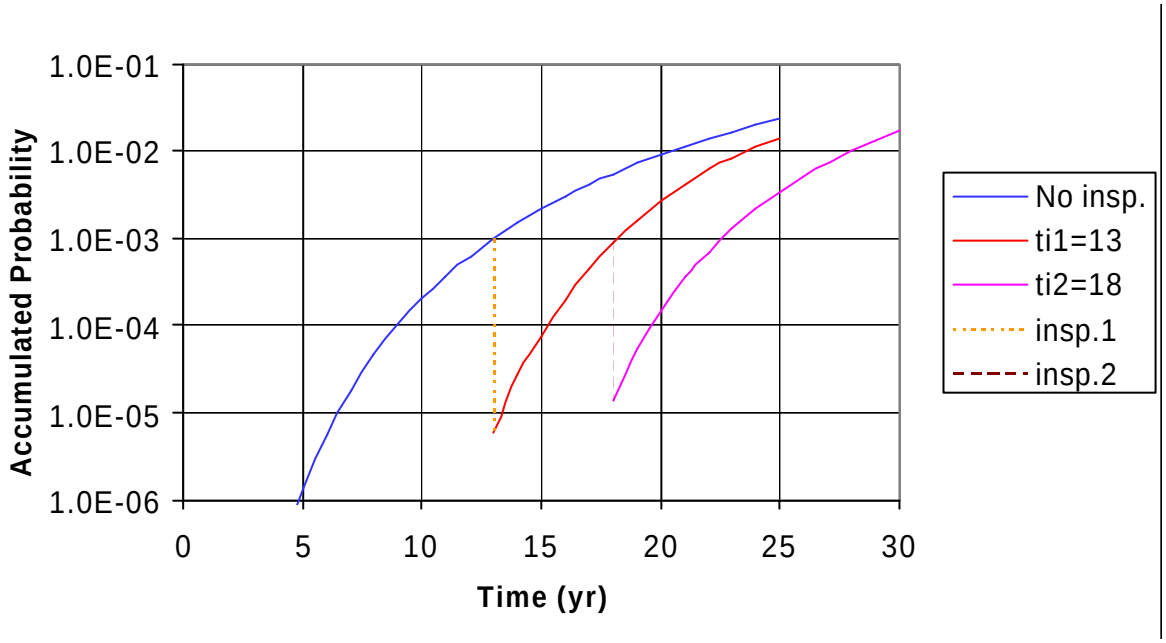

Figure 13 Illustration of part of an inspection plan with a target probability of 10^{-3}.

3.4 Optimisation

When the cost ratio of failure cost to inspection cost is 2.5, then it is cost-optimal to omit in-service inspections of the chain, in the present case study. This remains the case up to a cost ratio of about 90. The cost elements for this case are shown in Figure 14. The minimum cost is still found at target Pf=0.1, at which no inspections are required, but the failure risk cost now exceeds the inspection cost at this target.

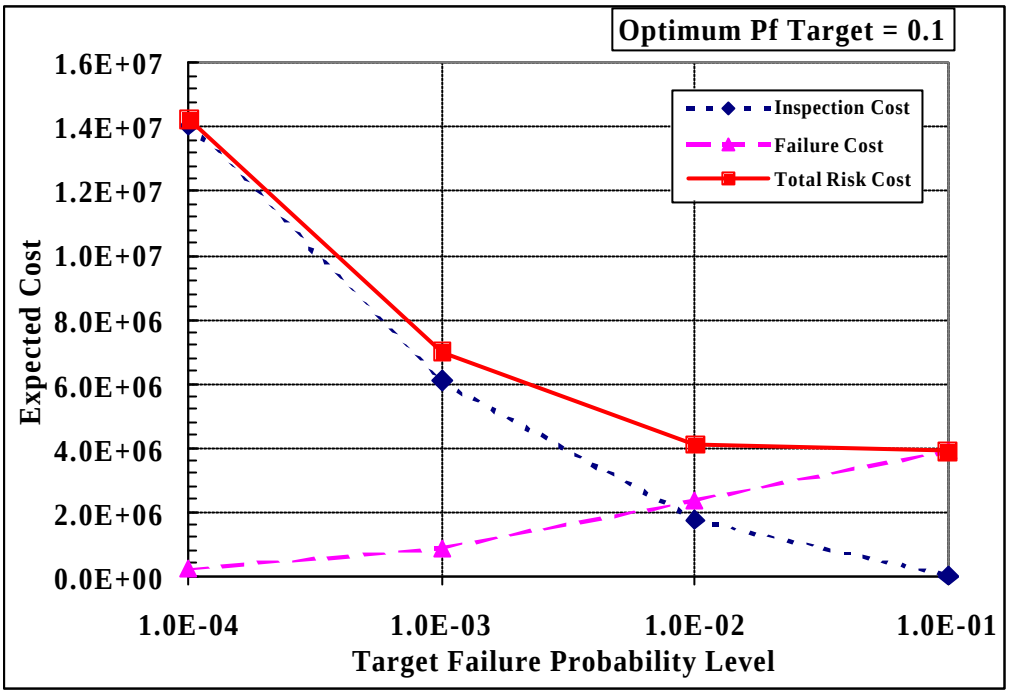

Figure 14 Cost elements plotted against target level for failure cost to inspection cost ratio of 90.

When the cost ratio is increased to 120, the optimal target is Pf=0.01, as shown in Figure 15. Now, one inspection is cost-optimal, after 21 years, as shown in Figure 16.

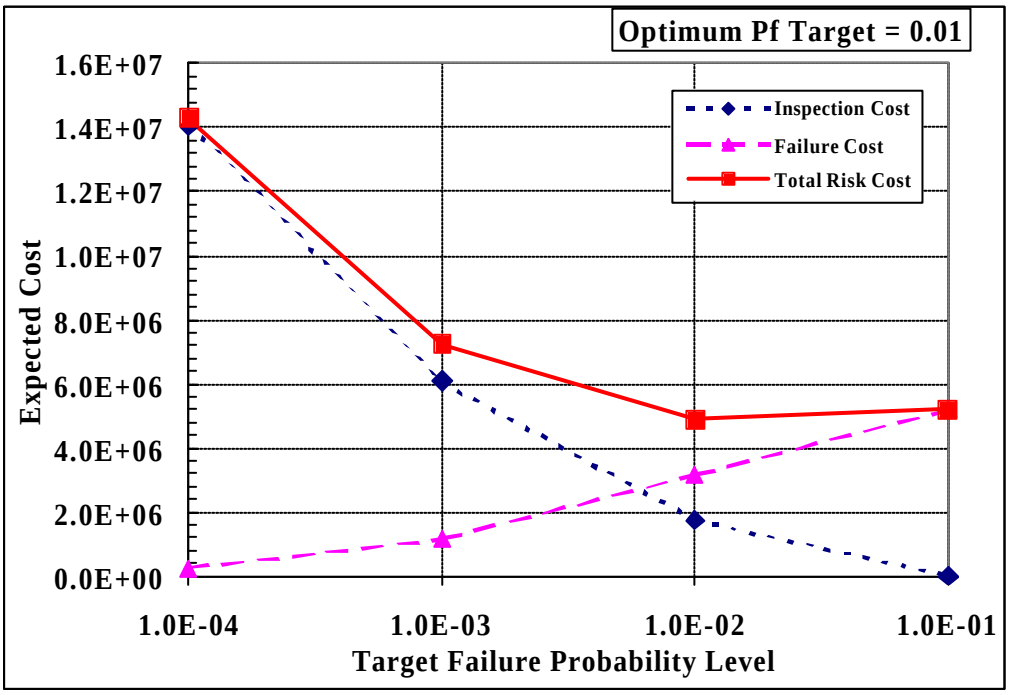

Figure 15 Cost elements plotted against target level for failure cost to inspection cost ratio of 120.

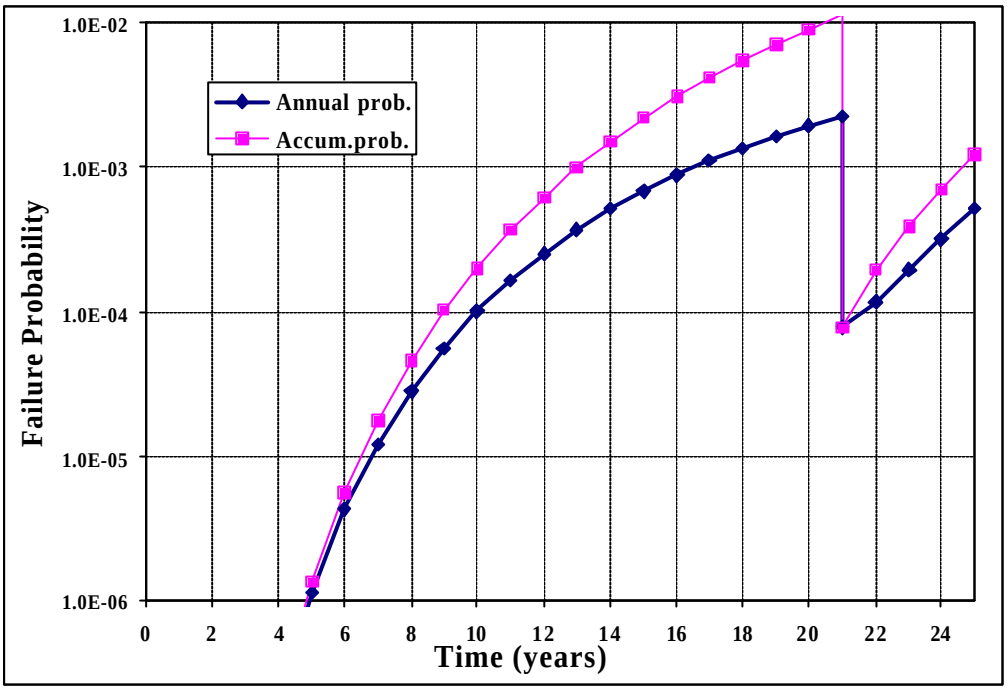

Figure 16 Updated failure probability with cost-optimal inspection plan for failure cost to inspection cost ratio of 120.

When the cost ratio is increased further to 1500, then the optimal target is Pf=0.0001, as shown in Figure 17. Now, six inspections are cost-optimal, with the first after 9 years, as shown in Figure 18.

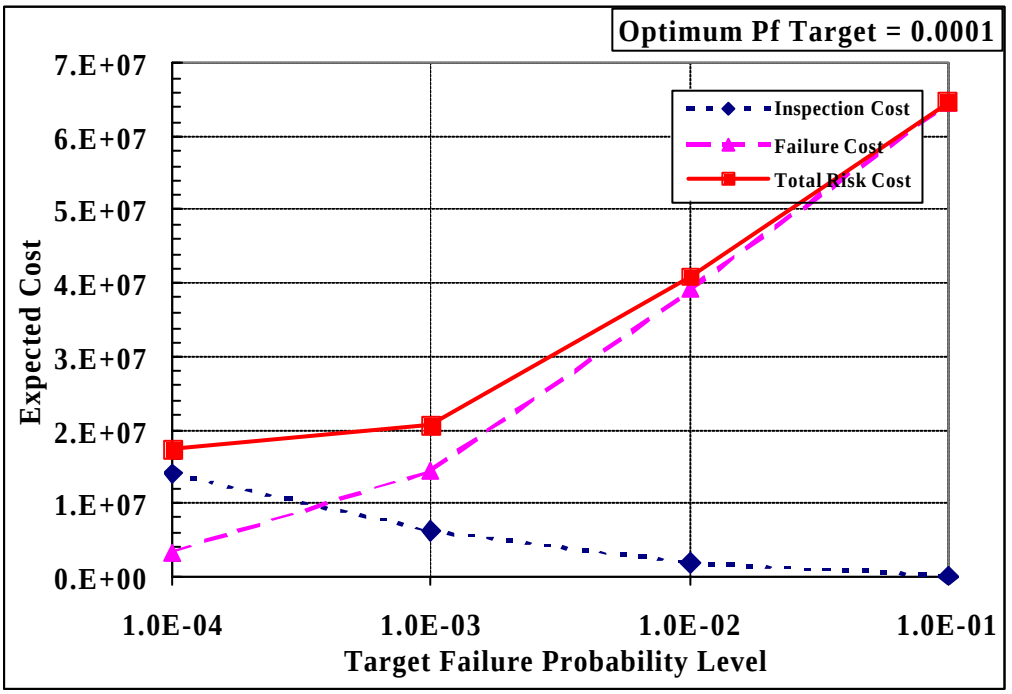

Figure 17 Cost elements plotted against target level for failure cost to inspection cost ratio of 1500.

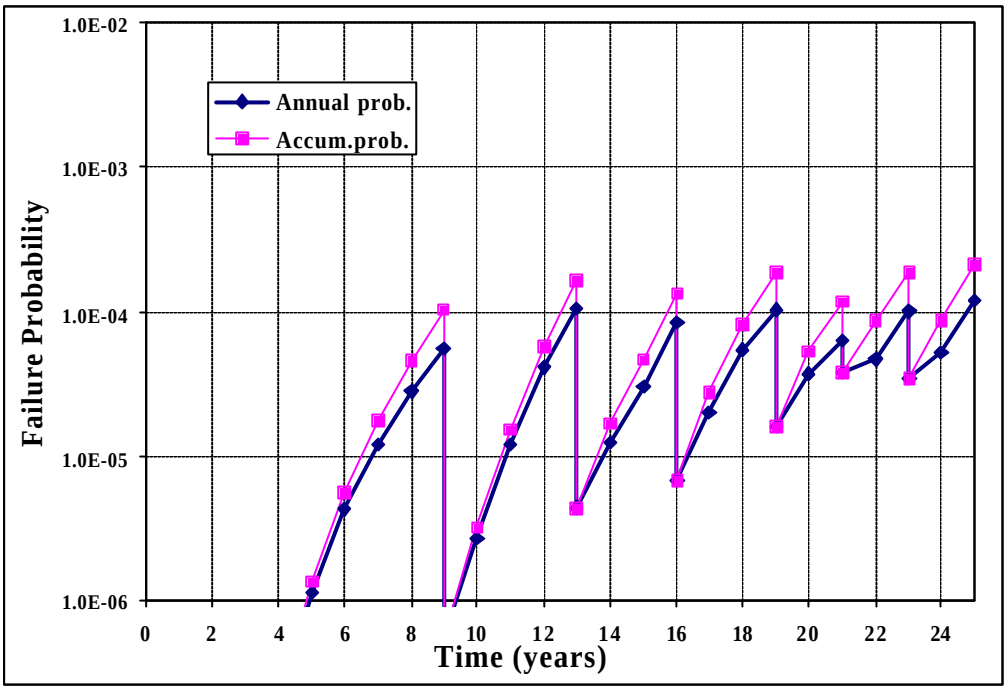

Figure 18 Updated failure probability with cost-optimal inspection plan for failure cost to inspection cost ratio of 1500.

4 Conclusion

A fatigue reliability analysis of a studless chain link has been developed on the basis of linear fracture mechanics, and calibrated against S-N data for this type of chain, in a saltwater environment. The reliability analysis has been extended from a single link to a chain segment, while taking account of the stochastic dependency (or correlation) between the chain links. Probabilistic updating of the fatigue reliability on the basis of results from chain inspections has been carried out, by comparing the predicted crack sizes with an appropriate probability of detection curve for magnetic particle inspection. A systematic series of reliability analyses have been made, with and without updating for inspection. These results have been combined with the cost of inspection and the risk cost of failure to derive a cost-optimal inspection plan.

In the present case study on a rather short and conservatively designed chain segment:

- it has been found to be preferable to inspect all links rather than the usual sample of links, if inspection is carried out,
- it is found to be cost-optimal to omit in-service inspections if a single line failure in fatigue does not lead to further line failures.

Note that the present analysis only addresses fatigue failure of chain due to normal cyclic loading. It does not take account of the effects of sub-standard chain quality or accidental damage to the chain. The model can be used to investigate the sensitivity of the results to some effects of this type, but they cannot be fully incorporated in the analysis because they are not adequately quantified. An initial inspection during installation, or early in the service life is usually good practice, to guard against such effects. Regular visual inspection of the

chain may also be advisable. Furthermore, an accidental limit state is included the design basis to ensure that the mooring system is designed with an allowance for line failures due to such effects.

A single mooring line failure is not normally expected to cause significant risk to the safety of personnel, or significant risk of pollution. This is not necessarily the case for mooring system failure. If there are significant risks of these types, then safety requirements usually take precedence over cost-optimal considerations. Hence, it may be useful to quantify the risk of a single line failure escalating to a mooring system failure. The particular scenario involved here implies that empirical statistics may not be suitable for this purpose, since a change in inspection procedure is involved, which tends to invalidate empirical data based on standard inspection procedures.

5 Acknowledgements

This application of risk-based inspection planning to mooring lines was originally suggested as a joint industry project, but failed to gain a sufficient number of sponsors. It has now been carried out on behalf of Statoil. Permission to publish this work is gratefully acknowledged. The material presented herein should not necessarily be taken to represent the views of Statoil or of DNV. Note also that some input data have been changed to separate the results presented here from the actual ship that was originally analysed. Cooperation from DNV colleagues Bjørn Klasen, Agnar Karlsen and Gudfinnur Sigurdsson is also gratefully acknowledged.

6 References

API, (1995), “Recommended Practice for Design and Analysis of Stationkeeping Systems for Floating Structures,” RP2SK, American Petroleum Institute, Washington D.C.

BSI (1999), “Guide on methods for assessing the acceptability of flaws in fusion welded structures,” BS 7910, British Standards Institution.

Det Norske Veritas, (2001), “Offshore Standard DNV-OS-E301, Position Mooring,” Høvik.

Couroneau, N., Royer, J., (1998), “Simplified model for the fatigue growth analysis of surface cracks in round bars under mode I,” Int. Journal of Fatigue, Vol.20, no. 10, pp.711-718.

Førli, O., (2000), “RBI for Offshore Structures – Service Development, POD curves for electromagnetic NDT,” memo no. forl/00aaabx1, DNV Materials Technology and Laboratories RN530, Høvik.

Klasén,B., Dillstrøm,P, (2001), private communication of results from stress analysis of a bar with flaws of various sizes.

Mathisen, J., (1999a), “Changes to DNV’s POSMOOR Rules, Based on the DEEPMOOR Project,” Seminar on Dynamic Positioning and Mooring of Floating Offshore Structures, Norwegian Soc. of Chartered Engineers, Sandefjord.

Mathisen, J., Hørte,T., Moe,V., Lian,W., (1999b), “DEEPMOOR – Design Methods for Deep water Mooring Systems, Calibration of a Fatigue Limit State,” Det Norske Veritas, report no. 98-3110, rev.no. 03, Høvik.

Pommier, S., Sakae, C., Murakami, Y., (1999), “An empirical stress intensity factor set of equations for a semi-elliptical crack in a semi-infinite body subjected to a polynomial stress distribution,” Int. Journal of fatigue, Vol.21, pp.243-251.

Okkenhaug, S., (2001), “DNV POSMOOR – New Edition 2001,” conference on Dynamic Positioning and Mooring of Floating Offshore Structures, Norwegian Society of Chartered Engineers, Kristiansand.

SESAM, (1996), “User’s Manual PROBAN General Purpose Probabilistic Analysis Program,” DNV Software report no. 92-7049, rev.no. 1, Høvik.

Sigurdsson, G., Lotsberg, I. & Landet, E., (2000), “Risk Based Inspection of FPSOs” , Int. Conf. on Offshore Mechanics and Arctic Engineering, OMAE'2000, New Orleans